Novel DOTA-Neurotensin Analogues for In-111 Scintigraphy and Ga-68 PET Imaging of Neurotensin Receptor-Positive Tumors

ARTICLE *in* BIOCONJUGATE CHEMISTRY · JUNE 2011

Impact Factor: 4.51 · DOI: 10.1021/bc200078p · Source: PubMed

9 AUTHORS, INCLUDING:

Faisal Alshoukr
French Institute of Health and Medical Resea…
10 PUBLICATIONS **63** CITATIONS
SEE PROFILE

A. Prignon
Pierre and Marie Curie University - Paris 6
15 PUBLICATIONS **100** CITATIONS
SEE PROFILE

Dirk A Tourwé
Vrije Universiteit Brussel
251 PUBLICATIONS **3,597** CITATIONS
SEE PROFILE

Jacques Barbet
French Institute of Health and Medical Resea…
256 PUBLICATIONS **5,947** CITATIONS
SEE PROFILE

Bioconjugate Chemistry

ARTICLE

pubs.acs.org/bc

Novel DOTA-Neurotensin Analogues for ^{111}In Scintigraphy and ^{68}Ga PET Imaging of Neurotensin Receptor-Positive Tumors

Faisal Alshoukr,[†,‡,§,Δ] Aurélie Prignon,[∥,Δ] Luc Brans,[⊥] Abdelhak Jallane,[†,‡,§] Sandra Mendes,[†,‡,§] Jean-Noël Talbot,[∥] Dirk Tourwé,[⊥] Jacques Barbet,[#,§] and Anne Gruaz-Guyon*[,†,‡,§]

[†]Inserm, U773, Paris, F-75018, France

[‡]Université Denis Diderot-Paris 7, UMR S773 Paris, F-75018, France

[§]CNRS, GDR 3260 Antibodies and therapeutic targeting, Tours, F-37032, France

[∥]Plateforme LIMP, IFR 65, Université Pierre et Marie Curie, Paris, F-75020, France

[⊥]Department of Organic Chemistry, Vrije Universiteit Brussel, Pleinlaan 2, B-1050 Brussels, Belgium

[#]Centre de Recherche en Cancérologie de Nantes-Angers, Inserm, Université de Nantes, U892, Nantes, F-44000, France

ABSTRACT: Overexpression of the high affinity neurotensin receptor 1 (NTSR1), demonstrated in several human cancers, has been proposed as a new marker for human ductal pancreatic carcinoma and as an independent factor for poor prognosis for ductal breast cancer, head and neck squamous cell carcinoma, and non-small cell lung cancer. The aim of the present study was to develop new DOTA-neurotensin analogues for positron emission tomography (PET) imaging with ^{68}Ga and for targeted radiotherapy with ^{90}Y or ^{177}Lu. We synthesized a DOTA-neurotensin analogue series. Two of these peptides bear two sequence modifications for metabolic stability: DOTA-NT-20.3 shares the same peptide sequence as the previously described DTPA-NT-20.3. In the sequence of DOTA-NT-20.4, the Arg^8-Arg^9 bond was N-methylated instead of the Pro^7-Arg^8 bond in DOTA-NT-20.3. An additional sequence modification was introduced in DOTA-LB119 to increase stability. A spacer was added between DOTA and the peptide sequence to increase affinity. Binding to HT29 cells, which express NTSR1, *in vivo* stability, and biodistribution of the various analogues were compared, and the best candidate was used to image tumors of various sizes with the microPET in mice. ^{111}In-DOTA-NT-20.3, in spite of a relatively high uptake in kidneys, showed specific tumor uptake and elevated tumor to other organ uptake ratios. High contrast images were obtained at early time points after injection that allowed tumor detection at a time interval postinjection appropriate for imaging with the short-lived radionuclide ^{68}Ga. ^{111}In-DOTA-NT-20.4 displayed inferior binding to HT29 cells and reduced tumor uptake. ^{111}In-DOTA-LB119 displayed at early time points a significantly lower renal uptake but also a lower tumor uptake than ^{111}In-DOTA-NT-20.3, although binding to HT29 cells was similar. ^{68}Ga-DOTA-NT-20.3 displayed higher tumor uptake than ^{68}Ga-DOTA-LB119 and allowed the detection of very small tumors by PET. In conclusion, DOTA-NT-20.3 is a promising candidate for ^{68}Ga-PET imaging of neurotensin receptor-positive tumors. DOTA-NT-20.3 may also be considered for therapy, as the yttrium-labeled peptide has higher affinity than that of the indium-labeled one. A prerequisite for therapeutic application of this neurotensin analogue would be to lower kidney uptake, for example, by infusion of basic amino acids, gelofusin, or albumin fragments, to prevent nephrotoxicity, as with radiolabeled somatostatin analogues.

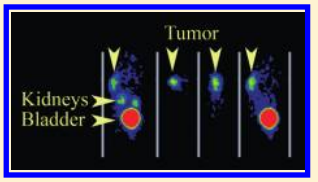

INTRODUCTION

During the past few years, several reports have pointed to the role of neurotensin and the high affinity neurotensin receptor 1 (NTSR1) in the progression of a variety of human cancers.[1] Neurotensin (NT) is a tridecapeptide which acts, in the central nervous system, as a neuromodulator involved in dopamine transmission, inhibition of food intake, hypothermia, and analgesia. In the periphery, neurotensin effects involve hypotension, decrease in gastric acid secretion, lipid digestion, gut motility, proinflammatory response, and also cell proliferation of a variety of normal or cancer cells such as pancreatic adenocarcinoma, colon, prostate, breast, and lung cancer cells.[1−4] Neurotensin exerts its trophic effects, in an endocrine, paracrine, or autocrine fashion, predominantly through NTSR1, but NTSR2 and particularly NTSR3 may also contribute to growth stimulation of normal and neoplastic tissues.[3] Overexpression of NTSR1 has been demonstrated in several human cancers such as pancreatic adenocarcinoma (75−88%),[5,6] invasive ductal breast cancer (91%),[7] non-small cell lung carcinoma (60%),[8] malignant mesothelioma (90%),[9] colon adenocarcinoma,[10] head and neck squamous cell carcinoma,[11] prostate cancer,[12] small cell lung carcinoma, Ewing's sarcoma, and meningioma.[13] Recent studies have suggested that increased NTSR1 expression contributes to the progression and aggressiveness of several tumors.[7,8,10,11] In addition, NTSR1 overexpression has been proposed as a new marker for human ductal pancreatic carcinoma [6] and as an independent factor for poor prognosis for ductal breast cancer,[14] head and neck squamous cell carcinoma,[11] and non-small cell lung cancer.[8]

Received: February 8, 2011
Revised: May 18, 2011
Published: June 12, 2011

Table 1. Peptide Sequence and Analytical Data

peptide	sequence	% purity	M+H$^+$ MALDI-TOF	M+H$^+$ calculated
NT	pGlu-Leu-Tyr-Glu-Asn-Lys-Pro-Arg-Arg-Pro-Tyr-Ile-Leu-OH			
NT(8−13)	H-Arg-Arg-Pro-Tyr-Ile-Leu-OH			
NT-20.3	Ac-Lys-Pro-Me-Arg-Arg-Pro-Tyr-Tle-Leu-OH			
DTPA-NT-20.3[a]	Ac-Lys(DTPA)-Pro-Me-Arg-Arg-Pro-Tyr-Tle-Leu-OH	>99	1473.83	1473.80
DOTA-NT-20.3	Ac-Lys(DOTA)-Pro-Me-Arg-Arg-Pro-Tyr-Tle-Leu-OH	98	1484. 83	1484.85
DOTA-NT-20.4	Ac-Lys(DOTA)-Pro-Arg-Me-Arg-Pro-Tyr-Tle-Leu-OH	>97	1484. 84	1484.85
DOTA-LB119[b]	Ac-Lys(Ahx-DOTA)-Pro-Me-Arg-Arg-Pro-Dmt-Tle-Leu-OH	>95	1627.08	1626.98

[a] Previously published.[19] [b] Ahx: aminohexanoic acid; Dmt: 2′,6′-dimethyltyrosine.

Radiolabeled neurotensin analogues could be used with scintigraphy or positron emission tomography (PET) for staging and/or prognostication, treatment follow-up, and further for internal radiotherapy of tumors overexpressing neurotensin receptors. The potential of radiolabeled peptide receptor ligands has been demonstrated by the role of somatostatin receptor ^{111}In-scintigraphy, which is nowadays a routine imaging modality in the diagnosis and staging of gastroenteropancreatic neuroendocrine tumors (GEPNETs), and by the therapy results obtained with ^{90}Y- and ^{177}Lu-labeled somatostatin analogues.[15,16]

We have previously developed DTPA-conjugated analogues of NT(8−13), the minimal sequence that mimics the effects of full-length NT,[17] and of NT(6−13).[18,19] Since neurotensin is rapidly degraded *in vivo*, sequence modifications were introduced to stabilize these molecules. An NT(6−13) analogue, DTPA-(^{111}In)-NT-20.3, may be considered a promising candidate for ^{111}In imaging of neurotensin receptor-positive tumors. This tracer showed specific tumor uptake *in vivo* and yielded high contrast on planar and SPECT tumor imaging in nude mice. In spite of a relatively high uptake in kidneys, uptake ratios between tumors and other normal organs including stomach, small intestine, and colon were high. Tumor was detected at early time points postinjection (30−60 min) on images obtained with ^{111}In-DTPA-NT-20.3. Such a time interval is appropriate for imaging with the short-lived radionuclide ^{68}Ga (half-life of 68 min). Indeed, ^{68}Ge/^{68}Ga generators, with a relatively long half-life that permits use over more than one year, have been made available. They provide ^{68}Ga independently of an on-site cyclotron. The generators make the labeling of peptides with this positron emitting radionuclide relatively easy by simple chelation.[20] They prompted the development of several ^{68}Ga-labeled radiopharmaceuticals, particularly peptide receptor ligands such as somatostatin, α-MSH, or bombesin analogues.[15,21−23] The superiority of PET imaging of somatostatin receptors with ^{68}Ga-labeled somatostatin derivatives over SPECT with ^{111}In-labeled pentetreotide has been reported in a number of publications.[24−27]

DTPA provides easy and stable peptide labeling with indium-111. However, labeling stability has been shown to be less satisfactory with other radioactive metals, particularly for yttrium-90 for therapy. The macrocyclic chelator 1,4,7,10-tetraazacyclododecane-*N*,*N*′,*N*″,*N*‴-tetraacetic acid (DOTA) is suitable for labeling with numerous radionuclide and is much more efficient in preventing leakage and subsequent bone marrow toxicity in targeted radionuclide therapy with yttrium-90.[28] DOTA-substituted peptides have also been used successfully for labeling with lutetium-177 and gallium-68. The aim of the present study was thus to develop a new DOTA conjugated neurotensin analogue series that would allow PET imaging with ^{68}Ga of neurotensin receptor-positive tumors, using DTPA-NT-20.3 as lead molecule. These DOTA-neurotensin analogues should also be suitable for labeling with ^{90}Y or ^{177}Lu in the aim of internal radiotherapy. Binding to HT29 cells, which express NTSR1, *in vivo* stability, and biodistribution of the various analogues were compared, and the best candidate was used to image tumors of various sizes with the microPET in mice.

MATERIALS AND METHODS

Cells. Experiments were performed with the HT29 human colorectal carcinoma cell line (ATCC, Rockville, USA). Cells were grown in DMEM (Gibco, France) supplemented with 10% fetal calf serum, 2 mM glutamine, and 50 μg/mL gentamycin at 37 °C in 5% CO_2.

Synthesis of the DOTA-NT Analogues. All reagents used for the synthesis were obtained from Sigma-Aldrich (Saint Quentin Fallavier, France, or Bornem, Belgium), Macrocyclics (Dallas, USA), Novabiochem (Läufelfingen, Switzerland), Bachem (Bubendorf, Switzerland), and RSP (Shirley, USA).

Sodium acetate 2 M was obtained from Hospira (Lake Forest, USA), absolute ethanol from Prolabo (Briare, France), trifluoroacetic acid from Supelco (Bellefont, USA). Water purified on Chelex resin from Biorad (St. Louis, USA) was used in all reactions.

The purity of the compounds was checked by HPLC on a Nucleosil C_{18} (5 μm, 100 Å, Shandon, France) reverse-phase column or on a Discovery BIO SUPELCO Wide Pore (5 μm, 300 Å, Sigma-Aldrich) column with a gradient of A, water (0.05% TFA), and B, CH_3CN (0.05% TFA), at a flow rate of 1.5 mL/min on a Waters apparatus.

The acetylated NT(6−13) analogues NT-20.3 (Ac-Lys-Pro-Me-Arg-Arg-Pro-Tyr-Tle-Leu-OH) and NT-20.4 (Ac-Lys-Pro-Arg-Me-Arg-Pro-Tyr-Tle-Leu-OH) were synthesized by NeoMPS (Strasbourg, France). 1,4,7,10-Tetraazacyclododecane-1,4,7-tris-(acetic acid)-10-acetic acid mono(*N*-hydroxysuccinimidyl ester) (DOTA-NHS ester) (Macrocyclics, Dallas, TX, USA) (5 equiv) was coupled to the lysine ε-NH_2 of NT-20.3 or of NT-20.4 (1 equiv) as described.[29] These DOTA-NT-20.3 and DOTA-NT-20.4 were purified by C_{18} reverse phase chromatography (5 μm, 100 Å, Nucleosil, Shandon, France) using a linear 150 min gradient (flow rate, 2 mL/min; A, H_2O/TFA(0.05%); B, acetonitrile/TFA(0.05%)) from 0% to 37% B. Coupling yields were approximately 85% for DOTA-NT-20.3 and 64% for DOTA-NT-20.4.

DOTA-LB119 was obtained starting from Ac-Lys(Dde)-Pro-Me-Arg(Pbf)-Arg(Pbf)-Pro-Dmt(Trt)-Tle-Leu-OWang resin. After deprotection of the Dde protection using $NH_2OH.HCl$/imidazole,[30] Fmoc-Ahx was coupled to the free ε-NH_2 group of Lys (DIC/HOBt) followed by Fmoc deprotection and coupling

dx.doi.org/10.1021/bc200078p |*Bioconjugate Chem.* 2011, 22, 1374–1385

of DOTA($OtBu$)$_3$ using HATU. The peptide was cleaved from the resin using TFA/H_2O/thioanisole/phenol/ethanedithiol (82.5:5:5:5:2.5) and purified by HPLC.

All DOTA-peptides were purified to at least 95% purity and identified by mass spectrometry (Table 1).

Radiolabeling. *^{111}In Labeling.* DTPA-NT-20.3 was labeled with ^{111}In as already described.[19] The DOTA-NT analogues (1 nmol) were labeled with indium-111 ($^{111}InCl_3$, 10−20 MBq, Covidien imaging, France) in 270 mM acetate, 27 mM citrate, buffer pH 4.5 during 25 min at 95 °C. Excess free indium was removed on a Sep-Pak cartridge (Waters Milford, USA). Radiochemical purity was confirmed by reverse-phase HPLC.

^{68}Ga Labeling. A fully automatic, PC-controlled, radiopharmaceutical synthesis device (SynChrom R&D, Raytest, Germany) was used for all labeling steps. ^{68}Ga ($t_{1/2}$ 68 min) was eluted from a ^{68}Ge/^{68}Ga-generator-system (IGG100, Eckert Ziegler, Berlin) in which ^{68}Ge ($t_{1/2}$ 270.8 d) was attached to a borosilicate glass column containing a titanium dioxide bed. The ^{68}Ga was eluted with 5 mL of 0.1 M hydrochloric acid. DOTA-peptide (25 nmol) in 290 μL 0.8 M sodium acetate was added to 300 MBq of $^{68}GaCl_3$ in 2 mL 0.1 M HCl. The reaction mixture (pH 3.5) was incubated at 95 °C for 8 min. Excess free ^{68}Ga was removed on a Sep-Pak cartridge (Waters Milford, USA). Radiochemical purity was confirmed by reverse-phase HPLC.

Determination of the IC_{50} of the DOTA-NT Analogues for Binding to NTSR1 in Living HT29 Cells and Kinetics of Activity Associated to or Internalized into Cells. The chelate formed by the nonradioactive metal (Me) and the DOTA-peptides (Me-DOTA-peptides) was obtained by incubation (25 min at 95 °C) of the DOTA-peptide (150 nmol in 150 μL water) with solutions of $InCl_3$, YCl_3, or $GaCl_3$ (1.5 μmol in 150 μL acetate 100 mM, citrate 10 mM, buffer, pH 5). IC_{50} for the binding to living HT29 cells was determined by competition between ^{125}I-labeled neurotensin (Perkin-Elmer, France) and the Me-DOTA-peptide chelate. HT29 cells (1.5×10^6 cells) were rinsed with 500 μL DMEM 0.2% BSA and incubated for 60 min at 37 °C with ^{125}I-labeled neurotensin (40 pM, 300 μL DMEM, 0.2% BSA, 0.8 mM 1,10-phenanthroline) in the presence of increasing concentrations of nonradioactive Me-DOTA-NT analogue. After washing the wells twice with ice-cold DMEM 0.2% BSA, cells were lysed in 500 μL 0.1 N NaOH and radioactivity was counted. Nonspecific binding was evaluated in the presence of 10^{-6} M neurotensin. Competition curves were analyzed with the *Equilibrium Expert* software.[31] All experiments were performed three times in triplicate.

Kinetic studies were performed with 0.5×10^{-9} M ^{111}In-DOTA-NT-20.3 or ^{111}In-DOTA-LB119 or 5×10^{-9} M ^{111}In-DOTA-NT-20.4 as above, except for the use of twelve-well plates (600 μL, 1.5×10^6 cells). At selected times, total radioactivity associated to the cells was evaluated as above. To determine the amount of internalized radioactivity, wells were incubated in DMEM/0.2% BSA, pH 2.0, for 15 min at 4 °C, to dissociate the surface-bound ligand. Internalized activity was then counted after washing and cell lysis. Nonspecific binding and internalization was evaluated in the presence of 10^{-6} M neurotensin. Results are expressed as the percentage of acid washed resistant activity, corresponding to specific binding, related to the activity specifically associated with the cells (I/B, mean ± sem).

***In Vivo* Metabolic Stability.** Female BALB/c mice ($n = 3-4$) were injected in the tail vein with ^{111}In-labeled DOTA-NT analogues (50 pmol). Mice were sacrificed 15 min after injection. Plasma and urine samples (50 μL) were added to 200 μL methanol and filtered. Then, methanol was evaporated under vacuum and the sample was analyzed by C_{18} RP-HPLC. Detection was performed with a radioactivity detector (HERM LB 500, Berthold, France). Elution was performed using, after 5 min at 0% B, a linear 15 min gradient from 0% to 35% B and a linear 25 min gradient from 35% to 50%; flow rate: 1.5 mL/min. The sample was also coinjected with fresh radioactive peptide to identify the peak corresponding to intact peptide. Under these conditions, the retention times of the peptides were 34.0 min for ^{111}In-DOTA-NT-20.3 and ^{111}In-DOTA-LB119 and 33.1 min for ^{111}In-DOTA-NT-20.4.

Biodistribution and Imaging Studies. All *in vivo* experiments were performed in compliance with the French guidelines for experimental animal studies and fulfill the UKCCCR guidelines for the welfare of animals in experimental neoplasia.

HT29 cells (6.7×10^5 cells) were inoculated subcutaneously in the flank of 6−8 week old athymic nu/nu male mice (Harlan, France). Biodistribution and imaging studies were performed two weeks later except as mentioned otherwise.

Biodistribution and Imaging Studies of ^{111}In-Labeled DOTA-NT Analogues. Mice were injected in the tail vein with ^{111}In-labeled DTPA-NT-20.3 (25−45 pmol) or ^{111}In-labeled DOTA-NT analogues (40−65 pmol, 0.5−0.7 MBq in 100 μL PBS 0.01% mouse serum albumin, except for mice dissected 49 h postinjection which received 500−900 pmol, 7−12 MBq) and sacrificed at different times. Blood, organs, and tumors were collected and weighed and radioactivity was counted. Injected activity was corrected for losses by subtraction of noninjected and subcutaneously injected material remaining in the animal tail. In blocked control experiments, each mouse received a coinjection of the labeled peptide and of its unlabeled counterpart (180 nmol NT-20.3 for DOTA-NT-20.3, Ac-Lys-Pro-Arg-Me-Arg-Pro-Tyr-Tle-Leu-OH for DOTA-NT-20.4, and Ac-Lys(Ahx)-Pro-Me-Arg-Arg-Pro-Dmt-Tle-Leu-OH for DOTA-LB119).

To estimate the areas under the time concentration curves (AUC) of the various peptides, biodistribution data collected at various time after injection were fitted using *WinSAAM*[32] to a pharmacokinetic model with two compartments to describe the distribution and elimination kinetics. Specific uptake in tumors and kidneys was modeled using one additional compartment for each tissue. Uptake data in tumor and kidneys were then fitted as the sum of the content of these additional compartments plus a fraction of the content of the central compartment of the model. To reduce the number of adjustable parameters, the volume of the central compartment was set to that of blood calculated as 9.5% of mean mouse body weight,[33] and the fractions of rapidly exchangeable fluid (blood + interstitial fluid) were set to 0.25 and to 0.39 for tumor and kidneys, respectively, as determined by Sung and co-workers[34] and Covell and co-workers.[35] The same model was used for all peptides. Addition of more compartments or adjusting the central compartment volume or the fractions of rapidly exchangeable fluid did not significantly improve data fitting. AUC were then calculated for blood, tumor, and kidneys by adding an accumulation compartment and extrapolating to 12 000 min.

^{111}In scintigraphic imaging was performed at the imaging platform of CEFI (Institut Claude Bernard, IFR 2, Paris). Mice under pentobarbital anesthesia were i.v. injected with ^{111}In-DOTA-NT analogues (500−900 pmol, 7−12 MBq) using a dedicated small animal Gamma Imager-S/CT system (Biospace Mesures) equipped with a parallel collimator (matrix 128 × 128,

with 15% energy windows centered on both indium-111 peaks at 171 and 245 keV). Planar anterior acquisitions were performed from 0 to 1 h, 1 to 1.5 h, 4.5 to 5.5 h, 24 to 25 h, and 48 to 49 h postinjection. Tumor to kidney activity ratio was evaluated using ROI surrounding the tumor and the right kidney. Radioactivity excretion in urine was determined from activity collected in the bladder 1.5 h postinjection.

Biodistribution and Imaging Studies with ^{68}Ga-Labeled DOTA-NT Analogues. Animals were injected in the retro-orbital sinus, under general anesthesia by isoflurane inhalation, with ^{68}Ga-DOTA-NT-20.3 (420 ± 30 pmol, 0.96 ± 0.08 MBq) or ^{68}Ga-DOTA-LB119 (450 ± 50 pmol, 1.2 ± 0.1 MBq) in 0.1 mL saline, 8 and/or 14 days after graft PET acquisitions were performed at the LIMP imaging platform (Hôpital Tenon, IFR 65 of Université Pierre et Marie Curie, Paris) with the Mosaic animal PET machine (Philips Medical systems, Cleveland, OH, USA). Static acquisitions were performed 45 min later with an exposure time of 10 min except otherwise mentioned.

Data were standardized with SUV units (standardized uptake value, g/mL). It is a widely used, simple PET quantifier, calculated as the ratio of radioactive concentration in a ROI surrounding the organ (MBq/mL) to the injected activity per animal body weight corrected from decay (MBq/g). Data were analyzed using *PETView* and Syntegra−Philips software (PETView; Philips Medical Systems, Bothell, WA).

Mice were sacrificed by cervical dislocation while under anesthesia one hour after injection. Blood, organs, and tumors were collected and weighed and radioactivity was counted. Tissue activity was decay-corrected.

For comparison, 9 days after inoculation of tumor cells, after a fasting period of 12 h, mice were injected intravenously with 6 to 10 MBq fluorodeoxyglucose (^{18}F) (FDG). Images were recorded one hour later with a 10 min acquisition time.

Statistical Analysis. Statistical analysis of differences in tissue uptake values was performed using unpaired *t* test for comparison between two groups or ANOVA analysis followed by Newman-Keuls' test for multiple comparisons. Differences of $p < 0.05$ were considered significant.

RESULTS

Synthesis of DOTA-NT Analogues. A series of NT (6−13) analogues that bear DOTA on the Lys^6 lateral chain were synthesized. The N-terminal end was acetylated to protect against amino-peptidases and to neutralize the positive charge of the α-NH$_2$ that favors renal accumulation.[36,37] Changes were introduced in the peptide sequence to protect the bonds between Arg^8 and Arg^9, Pro^{10} and Tyr^{11}, or Tyr^{11} and Ile^{12} against enzymatic degradation (Table 1). DOTA-NT-20.3 is the DOTA analogue of DTPA-NT-20.3, which provided, in a previous study, very encouraging ^{111}In targeting to neurotensin receptor-positive tumors.[19] This peptide was doubly stabilized by N-methylation of the Pro^7-Arg^8 bond and a Tle^{12} substitution. In DOTA-NT-20.4, the N-methylation was introduced at the Arg^8-Arg^9 bond instead of the Pro^7-Arg^8 bond in DOTA-NT-20.3.

We previously demonstrated that coupling of polyaminopolycarboxylate chelators such as DTPA dramatically decreases the affinity, unless the distance between the chelating agent and the NT(8−13) sequence that binds to the NTSR1 receptor is increased.[19] Therefore, we introduced an aminohexanoic acid spacer between DOTA and the peptide sequence in DOTA-LB119, an analogue of DOTA-NT-20.3 in which Tyr^{11} was replaced by 2′,6′-dimethyltyrosine (Dmt) to further stabilize the molecule.

All DOTA-peptides were purified to at least 95% purity and identified by mass spectrometry (Table 1).

Radiolabeling. ^{111}In-labeling yields of the DOTA-NT analogues were 82 ± 3% for DOTA(^{111}In)-NT-20.3, 79 ± 6% for DOTA(^{111}In)-NT-20.4, and 87 ± 2% for DOTA(^{111}In)-LB119. Very similar specific activities of about 11 MBq/nmol were obtained for the three peptides.

The decay-corrected labeling yield of ^{68}Ga obtained was 67 ± 9% with a specific activity of 2.5−4.5 MBq/nmol at the end of the labeling. The overall preparation time was 30 min.

After purification of the labeled compound on a reverse phase C$_{18}$ cartridge (Sep-Pak cartridge), the radiochemical purity of the ^{111}In- or ^{68}Ga-labeled analogues was checked by reverse-phase HPLC with a radioactivity detector: only one peak corresponding to the labeled peptide was detected on the chromatogram.

Binding Affinities. The IC$_{50}$ of the Me-DOTA-peptide chelates for the binding of ^{125}I-labeled neurotensin to living HT29 cells was measured after 60 min incubation at 37 °C. Since the peptides are rapidly internalized by target cells (see below), the determination of affinity constants for NTSR1 at 37 °C is not straightforward, and IC$_{50}$ values reflect the binding potential of the various peptides (Table 2). In-DOTA coupling had similar effects on affinity as In-DTPA, since In-DOTA-NT-20.3 IC$_{50}$ was similar to that of its In-DTPA-counterpart. Conversely, N-methylation of the Arg^8-Arg^9 bond, instead of the Pro^7-Arg^8 bond of In-DOTA-NT-20.3, increased the IC$_{50}$ by a factor of about 12 in In-DOTA-NT-20.4. This loss of affinity may be attributed to the importance of Arg^9 for binding to NTSR1, since replacement of this amino acid by citrulline decreases the affinity by about 100-fold.[38] In-DOTA-LB119 displayed an IC$_{50}$ similar to that of In-DOTA-NT20.3 in spite of the substitution of Tyr^{11} by Dmt, which decreased the affinity by a factor of 5 in the In-DTPA-NT(8−13) analogue series.[19] Most probably, the expected loss of affinity was compensated for by the introduction of an aminohexanoic acid spacer, between DOTA and the ε-NH2 of Lys^6 in In-DOTA-LB119.

The chelated metal also had an influence on the affinity of the complex. The yttrium complexes of DOTA-NT-20.3 and of DOTA-LB119 displayed lower IC$_{50}$ than the indium ones ($p < 0.01$). The IC$_{50}$ of the gallium chelate of DOTA-NT-20.3 was not significantly different from that of the indium complex, in opposition to the IC$_{50}$ decrease of the Ga-DOTA-LB119 as compared to In-DOTA-LB119 ($p < 0.001$).

Table 2. Affinity of Peptides for Binding to HT29 Cells

peptide	IC$_{50}$ (nM)
NT[a]	1.7 ± 0.4
NT-20.3[a]	2.2 ± 0.3
In-DTPA-NT-20.3[a]	16 ± 2
In-DOTA-NT-20.3	15 ± 1
Ga-DOTA-NT-20.3	14 ± 2
Y-DOTA-NT-20.3	5.6 ± 0.7
In-DOTA-NT-20.4	190 ± 20
In-DOTA-LB119	14.1 ± 0.7
Ga-DOTA-LB119	7.5 ± 0.7
Y-DOTA-LB119	9.9 ± 0.5

[a] For comparison, previously published.[19]

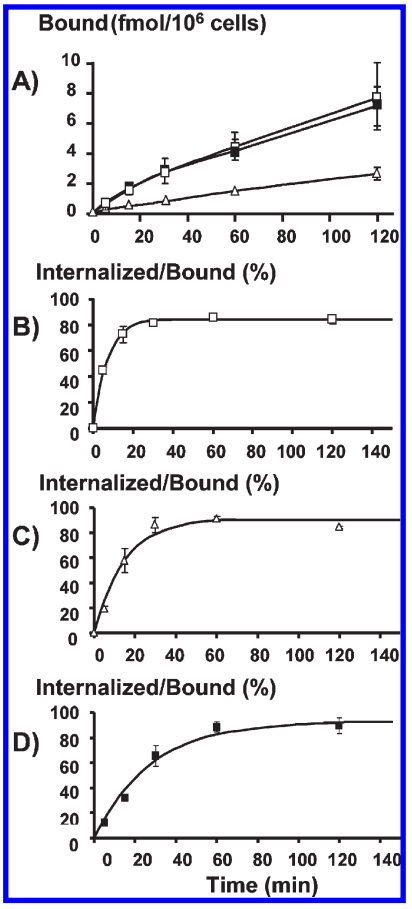

Figure 1. *In vitro* binding and internalization kinetics of ^{111}In-DOTA-peptides in HT29 cells. Panel A: Kinetics of specific radioactivity accretion to 1×10^6 HT29 cells at 37 °C (bound, fmol, mean ± sem) in the presence of 5×10^{-10} M labeled peptide. Each point is the average of four experiments performed in triplicate. Open squares: ^{111}In-DOTA-NT-20.3. Black squares: ^{111}In-DOTA-LB119. Triangles: ^{111}In-DOTA-NT-20.4. Panels B (^{111}In-DOTA-NT-20.3), C (^{111}In-DOTA-NT-20.4), and D (^{111}In-DOTA-LB119): Internalization kinetics. Results are expressed as the percentage of acid washed resistant activity, corresponding to specific binding, related to the activity associated with the cells (internalized/bound, mean ± SEM). Radioactivity, associated to cells or acid wash resistant, corresponding to nonspecific binding was evaluated in the presence of 10^{-6} M neurotensin. Solid line: results fitted with a monoexponential curve. Three experiments performed in triplicate.

Kinetics of *in Vitro* Radioactivity Binding and Internalization into HT29 Cells. As expected from their IC_{50}, the binding of ^{111}In-DOTA-NT-20.3 and of ^{111}In-DOTA-LB119 was not significantly different at every time point, and a significantly lower binding was observed for ^{111}In-DOTA-NT-20.4 after 15 min of incubation (Figure 1). The amount of ^{111}In-DOTA-peptide associated with cells that was internalized into cells increased rapidly with time reaching a 85 ± 2% plateau for ^{111}In-DOTA-NT-20.3, 91 ± 2% for ^{111}In-DOTA-NT-20.4, and 93 ± 2% for ^{111}In-DOTA-LB119 after less than 60 min.

***In Vivo* Peptide Catabolism.** The stability to enzymatic degradation was evaluated *in vivo*. The fraction of radioactivity associated to the intact ^{111}In-DOTA-peptides in plasma was determined 15 min after *iv* injection to BALB/c mice (Figure 2). Samples were analyzed by C_{18} RP-HPLC chromatography. Metabolites eluted at shorter retention times than the full-length radioactive peptide.

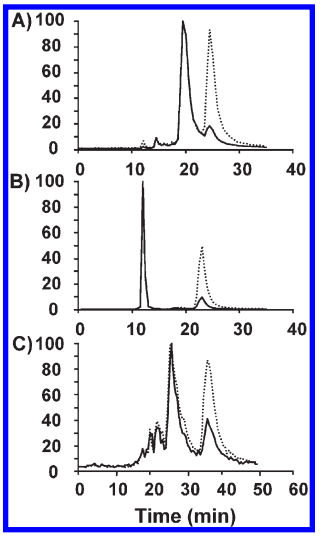

Figure 2. *In vivo* serum stability of ^{111}In-DOTA-peptides: representative C18 HPLC chromatograms of plasma samples collected 15 min postinjection to mice. (A) ^{111}In-DOTA-NT-20.3. (B) ^{111}In-DOTA-NT-20.4. (C) ^{111}In-DOTA-LB119. Solid line: plasma sample. Dotted line: coinjection of the sample with the radioactive control. Chromatograms were normalized to the highest metabolite peak.

There was no significant difference between the amount of intact peptide recovered in the plasma of mice injected with ^{111}In-DOTA-NT-20.3 (22 ± 1%) and ^{111}In-DOTA-LB119 (26 ± 3%), but ^{111}In-DOTA-NT-20.4 (16 ± 2%) was less stable than ^{111}In-DOTA-LB119 ($p < 0.05$). The fraction of activity (% ID/g) remaining in blood 15 min postinjection amounted to 6.1 ± 0.4%, 5.2 ± 0.2%, and 3.9 ± 0.8% for ^{111}In-DOTA-NT-20.3, ^{111}In-DOTA-NT-20.4, and ^{111}In-DOTA-LB119, respectively.

Biodistribution and Imaging Studies of the DOTA(^{111}In)-NT Peptides. Biodistribution studies of the neurotensin analogues ^{111}In-DTPA-NT-20.3 (Table 3), ^{111}In-DOTA-NT-20.3 (Table 4), ^{111}In-DOTA-NT-20.4 (Table 5), and ^{111}In-DOTA-LB119 (Table 6) were performed at various time points postinjection in male nude mice. Tumor accretion expressed as the percentage of injected dose per gram of tumor (%ID/g) showed no significant difference between ^{111}In-DTPA-NT-20.3 and ^{111}In-DOTA-NT-20.3 at any time postinjection, indicating similar tumor targeting efficacy of these two peptides. A slow tumor washout of both peptides was observed between 3 and 6 h, as already described for ^{111}In-DTPA-NT-20.3 in female nude mice. The renal uptake of these two peptides was not significantly different, except at 6 h postinjection ($P < 0.05$).

At early time points, ^{111}In-DOTA-NT-20.3 displayed a higher tumor uptake than ^{111}In-DOTA-LB119 (1 h $P < 0.001$ and 3 h $P < 0.05$), but ^{111}In-DOTA-LB119 tumor uptake decreased slowly with time and, from 6 to 24 h, no significant difference was observed between these two peptides. Renal accumulation of radioactivity was lower for ^{111}In-DOTA-LB119 than for ^{111}In-DOTA-NT-20.3 at early times postinjection ($P < 0.001$ at 1 h and $P < 0.05$ from 3 to 6 h). As a consequence, despite its lower tumor uptake, ^{111}In-DOTA-LB119 tumor to kidney uptake ratios were higher at 6 h ($P < 0.001$) postinjection than that of ^{111}In-DOTA-NT-20.3. ^{111}In-DOTA-NT-20.4 displayed a lower tumor uptake than ^{111}In-DOTA-NT-20.3 at every time point and than ^{111}In-DOTA-LB119 from 3 to 24 h, and a higher kidney uptake than these two peptides. As a consequence, the tumor to

Table 3. Tissue Distributions of ^{111}In-DTPA-NT-20.3 in Male Nude Mice Grafted with HT29 Cells

	^{111}In-DTPA-NT-20.3				
uptake (%ID/g)[a]	1 h $n = 4$	3 h $n = 4$	6 h $n = 6$	24 h $n = 4$	48 h $n = 3$
blood	0.13 ± 0.03	0.026 ± 0.004	0.023 ± 0.004	0.0076 ± 0.0008	0.0028 ± 0.0005
lungs	0.6 ± 0.3	0.11 ± 0.02	0.13 ± 0.04	0.044 ± 0.003	0.035 ± 0.003
liver	0.12 ± 0.01	0.093 ± 0.008	0.075 ± 0.009	0.049 ± 0.003	0.041 ± 0.002
spleen	0.13 ± 0.01	0.13 ± 0.02	0.10 ± 0.01	0.074 ± 0.005	0.064 ± 0.004
stomach[b]	0.14 ± 0.03	0.08 ± 0.02	0.15 ± 0.05	0.27 ± 0.08	0.033 ± 0.008
small intestine[b]	1.1 ± 0.4	0.5 ± 0.1	0.61 ± 0.09	0.38 ± 0.05	0.192 ± 0.005
large intestine[b]	0.5 ± 0.2	0.23 ± 0.02	1.4 ± 0.2	0.82 ± 0.13	0.15 ± 0.03
muscle	0.5 ± 0.4	0.14 ± 0.09	0.024 ± 0.005	0.023 ± 0.007	0.016 ± 0.004
bone	0.20 ± 0.06	0.10 ± 0.02	0.08 ± 0.01	0.044 ± 0.003	0.027 ± 0.004
kidney	7.8 ± 0.1	7 ± 2	2.8 ± 0.3	1.9 ± 0.3	1.5 ± 0.3
tumor	3.1 ± 0.4	2.0 ± 0.4	2.0 ± 0.2	0.86 ± 0.07	0.9 ± 0.1
			tumor(T)/organ		
T/blood	28 ± 7	75 ± 6	100 ± 20	110 ± 10	360 ± 90
T/kidney	0.40 ± 0.03	0.32 ± 0.03	0.72 ± 0.09	0.5 ± 0.1	0.64 ± 0.06
T/liver	26 ± 2	21 ± 3	27 ± 3	17.7 ± 0.5	23 ± 3
T/muscle	25 ± 9	40 ± 30	100 ± 10	50 ± 10	70 ± 10

[a] Uptake is expressed as the percentage of injected dose per gram of tissue (%ID/g). [b] Organs with their content.

Table 4. Tissue Distributions of ^{111}In-DOTA-NT-20.3 in Male Nude Mice Grafted with HT29 Cells

	^{111}In-DOTA-NT-20.3				
uptake (%ID/g)[a]	1 h $n = 7$	3 h $n = 11$	6 h $n = 7$	24 h $n = 4$	49 h $n = 3$
blood	0.36 ± 0.06	0.014 ± 0.002	0.006 ± 0.002	0.0028 ± 0.0003	0.0028 ± 0.0004
lungs	0.47 ± 0.04	0.14 ± 0.02	0.10 ± 0.01	0.062 ± 0.004	0.07 ± 0.01
liver	0.21 ± 0.02	0.13 ± 0.02	0.123 ± 0.008	0.085 ± 0.002	0.07 ± 0.01
spleen	0.19 ± 0.01	0.11 ± 0.01	0.113 ± 0.009	0.10 ± 0.01	0.16 ± 0.01
stomach[b]	0.13 ± 0.03	0.2 ± 0.1	0.09 ± 0.04	0.06 ± 0.01	0.020 ± 0.005
small intestine[b]	0.9 ± 0.1	0.52 ± 0.09	0.34 ± 0.06	0.32 ± 0.02	0.070 ± 0.003
large intestine[b]	0.39 ± 0.05	1.1 ± 0.3	1.5 ± 0.5	0.19 ± 0.02	0.058 ± 0.007
muscle	0.10 ± 0.02	0.027 ± 0.009	0.04 ± 0.01	0.0116 ± 0.0008	0.008 ± 0.001
bone	0.15 ± 0.02	0.10 ± 0.03	0.099 ± 0.007	0.030 ± 0.005	0.053 ± 0.002
kidney	7.6 ± 0.9	4.9 ± 0.4	5.2 ± 0.5	2.5 ± 0.1	0.86 ± 0.08
pancreas	0.095 ± 0.009	0.03 ± 0.01	0.030 ± 0.002	ND	ND
tumor	4.7 ± 0.8	2.5 ± 0.2	1.9 ± 0.2	1.3 ± 0.2	0.68 ± 0.09
			tumor(T)/organ		
T/blood	17 ± 5	170 ± 30	420 ± 90	500 ± 100	250 ± 30
T/kidney	0.63 ± 0.07	0.53 ± 0.05	0.35 ± 0.02	0.50 ± 0.04	0.78 ± 0.03
T/liver	22 ± 3	21 ± 2	17 ± 3	15 ± 1	11 ± 4
T/muscle	60 ± 20	130 ± 20	80 ± 20	110 ± 20	80 ± 20
T/pancreas	47 ± 8	90 ± 10	70 ± 10	ND	ND

[a] Uptake is expressed as the percentage of injected dose per gram of tissue (%ID/g). [b] Organs with their content.

kidney uptake ratio of this peptide was very low at every time postinjection.

Tumor uptake was receptor mediated, as shown by the dramatic decrease in tumor uptake when the radiolabeled ^{111}In-DOTA-peptides were coinjected with their unlabeled counterpart: 2.5 ± 0.2% vs 0.14 ± 0.02% ID/g for ^{111}In-DOTA-NT-20.3, 1.41 ± 0.05% vs 0.12 ± 0.03% for ^{111}In-DOTA-LB119, and 0.52 ± 0.07% vs 0.11 ± 0.01% for ^{111}In-DOTA-NT-20.4 ($p < 0.001$, 79−94% reduction, 3 h postinjection).

Radioactivity excretion in urine was fast, and more than 60% of the injected activity was recovered in the bladder 1.5 h after injection of ^{111}In-DOTA-NT-20.3 or ^{111}In-DOTA-LB119. Blood activity decreased rapidly for the three ^{111}In-DOTA-peptides, and low radioactivity uptake was observed in most nontumor organs, except in kidneys and, to some extent, in the gastrointestinal tract, particularly in small intestine and in colon. With the exception of kidneys, tumor to normal organ uptake ratios were high for ^{111}In-DOTA-NT-20.3 and, to a lesser extent,

Table 5. Tissue Distributions of ^{111}In-DOTA-NT-20.4 in Male Nude Mice Grafted with HT29 Cells

	^{111}In-DOTA-NT-20.4				
uptake (%ID/g)[a]	1 h $n = 4$	3 h $n = 4$	6 h $n = 4$	24 h $n = 4$	49 h $n = 3$
blood	0.27 ± 0.03	0.040 ± 0.003	0.037 ± 0.005	0.016 ± 0.005	0.0019 ± 0.0006
lungs	0.27 ± 0.02	0.10 ± 0.03	0.07 ± 0.01	0.06 ± 0.01	0.037 ± 0.001
liver	0.107 ± 0.007	0.076 ± 0.008	0.09 ± 0.01	0.071 ± 0.007	0.074 ± 0.007
spleen	0.097 ± 0.006	0.082 ± 0.006	0.070 ± 0.006	0.075 ± 0.009	0.08 ± 0.02
stomach[b]	0.18 ± 0.09	0.16 ± 0.09	0.062 ± 0.005	0.05 ± 0.02	0.0086 ± 0.0009
small intestine[b]	0.5 ± 0.3	0.12 ± 0.03	0.15 ± 0.05	0.090 ± 0.008	0.023 ± 0.003
large intestine[b]	0.20 ± 0.04	0.5 ± 0.3	0.36 ± 0.05	0.12 ± 0.02	0.033 ± 0.007
muscle	0.10 ± 0.02	0.04 ± 0.01	0.040 ± 0.008	0.023 ± 0.008	0.010 ± 0.002
bone	0.16 ± 0.05	0.09 ± 0.01	0.06 ± 0.01	0.035 ± 0.005	0.037 ± 0.008
kidney	9 ± 2	8 ± 1	9 ± 2	4.2 ± 0.8	1.7 ± 0.7
pancreas	0.044 ± 0.004	0.027 ± 0.002	0.022 ± 0.003	0.023 ± 0.003	ND
tumor	0.8 ± 0.1	0.52 ± 0.07	0.5 ± 0.1	0.33 ± 0.05	0.21 ± 0.08
			tumor(T)/organ		
T/blood	3.1 ± 0.8	13 ± 2	13 ± 3	40 ± 10	130 ± 80
T/kidney	0.095 ± 0.008	0.064 ± 0.005	0.053 ± 0.002	0.080 ± 0.007	0.2 ± 0.1
T/liver	7.2 ± 0.7	6.8 ± 0.7	5.4 ± 0.6	7 ± 2	2.8 ± 0.8
T/muscle	9 ± 1	14 ± 3	12 ± 3	26 ± 7	30 ± 10
T/pancreas	18 ± 4	20 ± 4	23 ± 5	21 ± 5	ND

[a] Uptake is expressed as the percentage of injected dose per gram of tissue (%ID/g). [b] Organs with their content.

Table 6. Tissue Distributions of ^{111}In-DOTA-LB119 in Male Nude Mice Grafted with HT29 Cells

	^{111}In-DOTA-LB119				
uptake (%ID/g)[a]	1 h $n = 7$	3 h $n = 4$	6 h $n = 4$	24 h $n = 3$	49 h $n = 3$
blood	0.38 ± 0.05	0.023 ± 0.002	0.0045 ± 0.0002	0.007 ± 0.002	0.0016 ± 0.0003
lungs	0.36 ± 0.03	0.106 ± 0.007	0.09 ± 0.01	0.06 ± 0.01	0.04 ± 0.01
liver	0.20 ± 0.01	0.151 ± 0.007	0.14 ± 0.02	0.080 ± 0.005	0.09 ± 0.03
spleen	0.153 ± 0.007	0.09 ± 0.01	0.076 ± 0.009	0.064 ± 0.003	0.10 ± 0.03
stomach[b]	0.28 ± 0.08	0.16 ± 0.04	0.5 ± 0.5	0.08 ± 0.01	0.024 ± 0.004
small intestine[b]	1.1 ± 0.1	0.67 ± 0.08	0.7 ± 0.1	0.35 ± 0.05	0.084 ± 0.005
large intestine[b]	0.4 ± 0.1	1.5 ± 0.5	1.2 ± 0.8	0.16 ± 0.03	0.101 ± 0.006
muscle	0.09 ± 0.01	0.021 ± 0.005	0.05 ± 0.02	0.010 ± 0.003	0.015 ± 0.007
bone	0.15 ± 0.04	0.05 ± 0.01	0.07 ± 0.02	0.05 ± 0.01	0.05 ± 0.02
kidney	3.4 ± 0.2	2.4 ± 0.2	2.2 ± 0.2	1.04 ± 0.07	0.6 ± 0.1
pancreas	0.081 ± 0.008	0.0217 ± 0.0008	0.018 ± 0.001	0.0180 ± 0.0006	0.013 ± 0.002
tumor	1.8 ± 0.1	1.41 ± 0.05	1.4 ± 0.2	1.0 ± 0.3	0.46 ± 0.06
			tumor(T)/organ		
T/blood	6 ± 1	63 ± 7	300 ± 40	160 ± 60	330 ± 90
T/kidney	0.55 ± 0.05	0.60 ± 0.05	0.63 ± 0.06	0.9 ± 0.2	0.74 ± 0.07
T/liver	9.0 ± 0.7	9.4 ± 0.4	10 ± 2	12 ± 3	6 ± 1
T/muscle	24 ± 7	80 ± 10	80 ± 40	130 ± 70	40 ± 10
T/pancreas	25 ± 4	65 ± 2	75 ± 7	50 ± 10	37 ± 3

[a] Uptake is expressed as the percentage of injected dose per gram of tissue (%ID/g). [b] Organs with their content.

for ^{111}In-DOTA-LB119. For example, tumor to blood amounted to 170 ± 30% and 63 ± 7%, respectively, tumor to muscle 130 ± 20% and 80 ± 20%, tumor to pancreas 90 ± 10% and 65 ± 2%, and tumor to liver 21 ± 2% and 9.4 ± 0.4% at three hours postinjection (Tables 4 and 6). Some excretion by the digestive route was also observed: 55 ± 8% and 60 ± 10% of the radioactivity in the stomach and 76 ± 8% and 79 ± 2% in the colon were associated to the organ content for ^{111}In-DOTA-NT-20.3 and ^{111}In-DOTA-LB119, respectively, at 3 h postinjection. Nevertheless, tumor to stomach (32 ± 8% at 3 h postinjection), to small intestine (7 ± 1%), and to colon (4 ± 1%) ratios were quite high for ^{111}In-DOTA-NT-20.3. They were somewhat

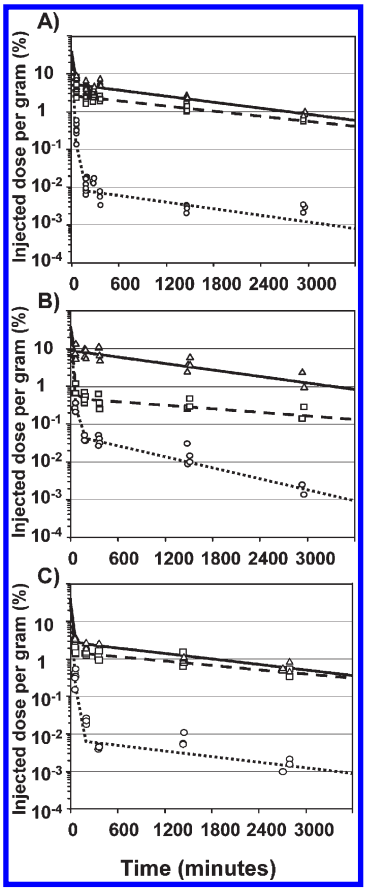

Figure 3. Biodistribution kinetics of ^{111}In-DOTA-peptides in tumor-bearing nude mice. Mice were injected with ^{111}In-DOTA-NT-20.3 (panel A), ^{111}In-DOTA-NT-20.4 (panel B), or ^{111}In-DOTA-LB119 (panel C) and sacrificed at selected time intervals. Blood sample (circles), tumors (squares), and right kidneys (triangles) were weighed and counted, and the activity was expressed as %ID/g. The three kinetics were fitted simultaneously using the same pharmacokinetic model as described in Materials and Methods, and the fitted curves for blood (dotted line), tumor (dashed line), and right kidney (solid line) are shown in the graphs as semilogarithmic plots.

lower for ^{111}In-DOTA-LB119: 10 ± 2%, 2.2 ± 0.3%, and 1.2 ± 0.3%, respectively. Some of the radioactivity accretion in the intestines was receptor-mediated, since after removal of their content, the radioactivity uptake was significantly reduced in small intestine (0.171 ± 0.008% vs 0.082 ± 0.007% ID/g for ^{111}In-DOTA-20.3 and 0.68 ± 0.01% vs 0.17 ± 0.04% ID/g for LB119, $p < 0.001$) and in colon (0.4 ± 0.1% vs 0.09 ± 0.02%, $p < 0.05$, and 0.7 ± 0.1% vs 0.16 ± 0.06% ID/g, $p < 0.01$, respectively), when the tracer was coinjected with an excess of unlabeled peptide.

Comparison between organ uptakes of different peptides at selected times postinjection hardly reflects irradiation doses delivered to these organs over time for a therapeutic injection of radiolabeled peptides. Then, for a preliminary evaluation of the potential of these peptides for targeted radiotherapy, areas under the time−activity curves (AUC expressed as %ID/g.min) were calculated after simultaneously fitting the activity biodistribution data for blood, tumor, and kidney to a multicompartmental model. The same, relatively simple model was used for all peptides with two compartments to describe the blood pharmacokinetic and one additional compartment to describe tumor and kidney uptake kinetics. The addition of a fraction of the central compartment, calculated on the basis of published data for the fractions of blood and interstitial fluid contained in tumors and normal organs,[34,35] to these tissues considerably improved data fitting. A total of seven parameters were thus adjusted to simultaneously fit the biodistribution data in blood, tumor, and kidneys. Good fitting was obtained in all cases (Figure 3, Table 7); however, it should be kept in mind that the kinetics reflect the total activity present in the tissues, responsible for tissue irradiation, and not the intact radiolabeled peptide, which is quickly catabolized. The estimated values for these parameters were rather similar for all peptides with subtle changes explaining the differences in pharmacokinetics.

Table 7. Area under Curves for Tumor, Kidneys, and Blood

peptide	tumor AUC[a]	kidney AUC[a]	blood AUC[a]
^{111}In-DTPA-NT-20.3	6743	10767	464
^{111}In-DOTA-NT-20.3	5463	9210	500
^{111}In-DOTA-LB-119	3687	5163	514
^{111}In-DOTA-NT-20.4	1618	13774	492

[a] Area under curve (AUC) are expressed as %ID/g.min.

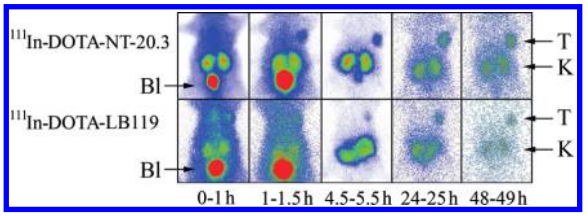

Figure 4. ^{111}In-DOTA-NT-20.3 and ^{111}In-DOTA-LB119 planar images of male nude mice grafted with HT29 cells. Planar anterior acquisitions were performed from 0 to 1 h, 1 to 1.5 h, 4.5 to 5.5 h, 24 to 25 h, and 48 to 49 h postinjection under anesthesia. Bl: bladder. K: kidney. T: tumor. Tumor weight: 167 mg for ^{111}In-DOTA-NT-20.3 and 196 mg for ^{111}In-DOTA-LB119.

Blood clearances were pretty close for all peptides; however, as judged by the AUC, tumor uptake was similar for ^{111}In-DTPA-NT-20.3 and ^{111}In-DOTA-NT-20.3, lower for ^{111}In-DOTA-LB119, and still lower for ^{111}In-DOTA-NT-20.4. Kidney uptake was lower for ^{111}In-DOTA-LB119, higher for ^{111}In-DTPA-NT-20.3 and ^{111}In-DOTA-NT-20.3, and even higher for ^{111}In-DOTA-NT-20.4. These resulted in similar tumor/kidney AUC ratios (0.6 to 0.7) for ^{111}In-DTPA-NT-20.3, ^{111}In-DOTA-NT-20.3, and ^{111}In-DOTA-LB119 and in a much lower value for ^{111}In-DOTA-NT-20.4 (0.1). The IC_{50} of the yttrium complex of DOTA-NT-20.3 is 2-fold lower than that of the indium one ($p < 0.01$).Then, one can expect that tumor AUC and so tumor to kidney AUC ratio may be higher with ^{90}Y- than ^{111}In-labeled DOTA-NT-20.3.

Planar images of mice grafted with HT29 cells were recorded from 1 to 48 h, after injection of ^{111}In-DOTA-NT-20.3 or ^{111}In-DOTA-LB 119 (Figure 4). There was a clear visualization of the tumor at early time points in mice injected with ^{111}In-DOTA-NT-20.3. At late time points, the tumor could be clearly detected with the two peptides. These results were consistent with biodistribution data and tumor to organ uptake ratios. Kidneys and bladder were the only other sites of visible activity accumulation. The activity ratio between tumor and kidneys was 0.47 ± 0.03% at 1 h and 0.69 ± 0.07% at 24 h for ^{111}In-DOTA-NT-20.3

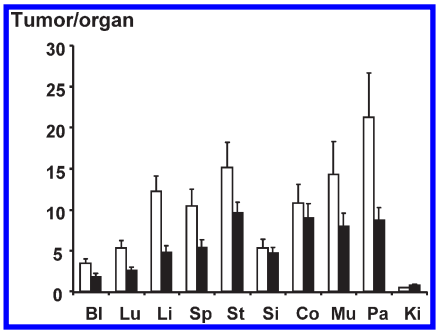

Figure 5. Tumor to normal organ uptake ratios obtained 1 h after injection of ^{68}Ga-DOTA-NT-20.3 (420 ± 30 pmol, 0.96 ± 0.08 MBq) or ^{68}Ga-DOTA-LB119 (450 ± 50 pmol, 1.2 ± 0.1 MBq) in male nude mice, grafted with HT29 cells. Bl: blood. Lu: lung. Li: liver. Sp: spleen. St: stomach. Si: small intestine. Co: colon. Mu: muscle. Pa: pancreas. Ki: kidney.

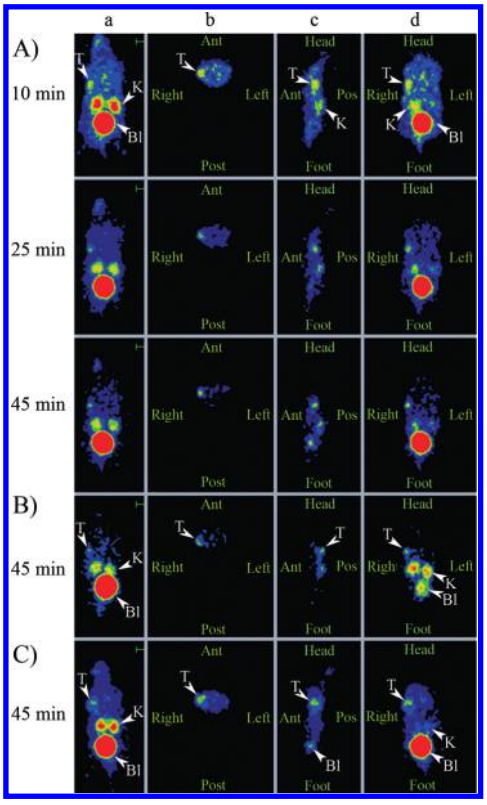

Figure 6. TEP imaging of male nude mice, grafted with HT29 cells in the right flank, injected with ^{68}Ga-DOTA-NT-20.3: (A) images were recorded at different time points after injection of ^{68}Ga-DOTANT-20.3; in the same mouse (tumor volume 40 mm^3), no tumor was detectable on ^{18}F-FDG PET images performed 24 h later; (B) and (C) images recorded 45 min after ^{68}Ga-DOTA-NT-20.3 injection (tumor volumes: 22 and 288 mm^3). Imaging was performed seven (A and B) or twelve days (C) after cell graft. The acquisition time was 10 min a = Maximum Intensity Projection (MIP), frames: b = axial, c = sagittal, and d = coronal. Bl: Bladder. K: Kidney. T: Tumor. ant: anterior. pos: posterior.

(tumor weight: 0.15 ± 0.04% g), 0.45 ± 0.05% and 0.50 ± 0.01% for ^{111}In-DOTA-LB119 (tumor weight: 0.20 ± 0.05% g).

Biodistribution and PET Imaging with ^{68}Ga-DOTA-NT-20.3 and ^{68}Ga-DOTA-LB119. Biodistribution studies were performed 1 h after injection of ^{68}Ga-DOTA-NT20.3 (420 ± 30 pmol, 0.96 ± 0.08 MBq) or ^{68}Ga-DOTA-LB119 (450 ± 50 pmol, 1.2 ± 0.1 MBq). No significant difference was observed between tumor uptake of ^{68}Ga-labeled and ^{111}In-labeled DOTA-NT-20.3, but, probably due to its higher affinity, ^{68}Ga-DOTA-LB119 tumor uptake was significantly increased as compared to ^{111}In-DOTA-LB119 (50% increase, $P < 0.05$). Nevertheless, the tumor uptake of ^{68}Ga-DOTA-NT20.3 was higher than that of ^{68}Ga-DOTA-LB119 ($P < 0.05$).

As observed for the ^{111}In complexes the renal accretion of ^{68}Ga-DOTA-LB119 was lower than that of ^{68}Ga-DOTA-NT20.3 ($P < 0.05$), and for both ^{68}Ga-labeled peptides, the renal uptake was similar to that of the ^{111}In-labeled ones. Tumor to normal tissue uptake ratios were similar or higher for ^{68}Ga-DOTA-NT20.3 as compared to ^{68}Ga-DOTA-LB119 except for kidneys (0.46 ± 0.06% vs 0.79 ± 0.07%) (Figure 5).

High contrast images were obtained with ^{68}Ga-DOTA-NT20.3, which allowed the visualization of very small tumors (Figure 6). As shown in Figure 6, 22 and 40 mm^3 tumor grafts could be easily detected as soon as 45 min after ^{68}Ga-DOTA-NT20.3 injection (10 min acquisition). The tumor SUV_{max} 45 min after ^{68}Ga-DOTA-NT-20.3 injection amounted to 0.9 ± 0.1 and the tumor to kidney SUV_{max} ratio was 0.6 ± 0.1. Tumor was not detectable on FDG PET images (not shown).

DISCUSSION

Since radiolabeled neurotensin analogues may be valuable tools for both imaging and therapy of neurotensin receptor-positive tumors, a number of radiolabeled neurotensin analogues, stabilized against enzymatic degradation *in vivo* by changes in the peptide sequence, has been described in the literature. In a series of peptides bearing (N^{α}His)Ac, a chelator of ^{99m}Tc and ^{188}Re, NT-XIX, an NT(8−13) analogue, displayed the most promising properties to target these radionuclides *in vivo*, with low kidney uptake, and reduction of tumor mass was observed after treatment with the rhenium-188-labeled peptide.[39,40] Nevertheless, some intestine uptake may be a source of background for imaging and of toxicity for therapeutic applications. Polyaminopolycarboxylate chelators, such as DTPA or DOTA, coupled to somatostatin analogues have been used with success to deliver various radiometals, including ^{111}In, ^{68}Ga, ^{90}Y, or ^{177}Lu, to somatostatin receptor-positive tumors, such as gastroenteropancreatic neuroendocrine tumors (GEPNETs). PET imaging with [^{68}Ga-DOTA^0,Tyr^3]octreotate or [^{68}Ga-DOTA^0,Tyr^3]octreotide has been reported to achieve higher diagnostic efficacy than SPECT with ^{111}In-labeled analogues.[24−27] In addition, therapy with [^{90}Y-DOTA^0,Tyr^3]octreotide and [^{177}Lu-DOTA^0,Tyr^3]octreotate provided symptomatic improvement, tumor regression, improved quality of life, and a benefit in overall survival.[15,16] Several DTPA and DOTA neurotensin analogues have been developed to target these radionuclides to tumors overexpressing neurotensin receptors.[18,41,42] However, these radiolabeled peptides showed moderate tumor uptake and comparably high kidney uptake. We recently reported the encouraging results obtained with a new DTPA-neurotensin(6−13) analogue, DTPA-NT-20.3, which displayed improved uptake ratio between tumor and kidneys, superior to previously published DTPA and DOTA neurotensin analogues.[19] High-quality planar scintigraphy and SPECT images were obtained after a short delay, compatible with the use of the short-lived radionuclide ^{68}Ga for PET imaging.

A macrocyclic chelator, such as DOTA, is necessary for targeted radionuclide therapy with ^{90}Y, since *in vivo* leakage of this radionuclide from DTPA complexes leads to bone marrow toxicity.[28] For PET imaging, the *in vivo* stability of ^{68}Ga-DTPA chelates remains a matter of controversy. Then, the aim of the present study was to design new DOTA-substituted neurotensin analogues suitable for ^{68}Ga PET imaging and possibly for ^{90}Y or ^{177}Lu targeted radiotherapy of neurotensin-receptor-positive tumors.

In the three synthesized DOTA-peptides, a Tle^{12} substitution was introduced to protect the bond between Tyr^{11} and Ile^{12}. Since positive charges increase renal uptake,[36,37] the α-NH_2 was neutralized by acetylation, which also protected the peptides against aminopeptidases. In DOTA-NT-20.3, which shares the same peptide sequence with DTPA-NT-20.3, an N-methylation of the Pro^7-Arg^8 bond was introduced for stability. In the triple-stabilized DOTA-LB119, Tyr^{11} was substituted with Dmt and a spacer was introduced between the peptide and the chelator in order to reduce the affinity loss induced by polyaminopolycarboxylate coupling, which we previously observed.[19] In DOTA-NT-20.4, the Arg^8-Arg^9 bond was protected by an N-methylation.

The properties of the ^{111}In labeled DOTA-peptides were evaluated and compared to those of ^{111}In-DTPA-NT-20.3. The affinity decrease induced by DOTA coupling is similar to that observed with DTPA, as indicated by the similar IC_{50} of these two peptides. As already observed for ^{111}In-DTPA-NT-20.3, the DOTA analogue rapidly internalizes *in vitro*. Biodistribution of both peptides was very similar in male nude mice grafted with HT29 cells. Circulating activity decreased rapidly, and high tumor to blood uptake ratios were obtained at early times postinjection. Tumor uptakes of both peptides were not significantly different at any time point and decreased quite slowly with time. Uptake in normal organs was low, leading to high tumor to organs ratio except in kidneys.

The three ^{111}In-DOTA-peptides exhibited receptor mediated tumor targeting, abolished by coinjection of their unlabeled counterpart. N-Methylation of the Pro^7-Arg^8 or of the Arg^8-Arg^9 bonds was similarly effective for *in vivo* stabilization, as shown by the stability results obtained with ^{111}In-DOTA-NT-20.3 and ^{111}In-DOTA-NT-20.4. Probably due to its lower affinity, tumor uptake of ^{111}In-DOTA-NT-20.4 was lower than the two other ^{111}In-DOTA-analogues. Unexpectedly, renal accumulation of this peptide was also higher. Although ^{111}In-DOTA-NT-20.3 and ^{111}In-DOTA-LB119 displayed similar stability and IC_{50}, the tumor uptake of this last peptide was significantly lower at early time points. Renal uptake was also lower at early time points for ^{111}In-DOTA-LB119, as already observed for Dmt^{11} substituted (N^{α}His)Ac-NT(8−13) analogues.[39] In agreement with the biodistribution studies, high contrast images were obtained with ^{111}In-DOTA-NT-20.3 with a clear detection of tumors at early time points.

Since tumor grafts were detected at early time points postinjection with ^{111}In-DOTA-LB119 and particularly ^{111}In-DOTA-NT-20.3, these peptides were further evaluated for ^{68}Ga targeting. Radiolabeling was obtained in good yields with ^{68}Ga, and no free ^{68}Ga was detected after purification. The specific activities obtained allowed the injection of less than 500 pmol per mouse for PET imaging, in order to minimize the saturation of tumor neurotensin receptors. For both peptides, uptake in normal organs, 1 h postinjection, was low except in kidneys. ^{68}Ga-DOTA-NT-20.3 provided reasonably high tumor uptake, higher than that of ^{68}Ga-DOTA-LB119. Very small tumor masses (20−40 mm^3) could be detected with ^{68}Ga-DOTA-NT-20.3 at 45 min after injection.

Metal complexation had an influence on the IC_{50} of the DOTA-peptides. Effects observed with gallium differed according to the peptide. No significant difference was observed with DOTA-NT-20.3, but it enhanced DOTA-LB119 affinity as compared to indium, and the tumor uptake of ^{68}Ga-DOTA-LB119 was significantly increased (by 50%). Yttrium significantly decreased the IC_{50} of both peptides. Such an affinity difference induced by the incorporated metal has already been described in the literature for DOTATOC[43] and bombesin analogues.[44]

CONCLUSION

In summary, in spite of a relatively high uptake in kidneys, ^{111}In-DOTA-NT-20.3 showed specific tumor uptake, provided elevated tumor to other organ uptake ratios, particularly tumor to intestine, and high contrast images at early time points after injection. A very low background in normal tissues, except kidneys, was obtained by PET imaging with ^{68}Ga-DOTA-NT-20.3 which allowed the detection of very small tumors. DOTA-NT-20.3 may be considered a promising candidate for ^{68}Ga-PET imaging of neurotensin receptor-positive tumors, such as pancreatic adenocarcinoma, invasive ductal breast cancer, and non-small cell lung carcinoma. The high affinity observed for the yttrium complex of DOTA-NT-20.3, higher than that of the indium one, suggests that targeting ^{90}Y with this peptide may ensure a higher tumor uptake than with ^{111}In. A prerequisite for therapeutic application of this neurotensin analogue would be to lower kidney uptake, for example, by infusion of basic amino acids, gelofusin, or albumin fragments, to prevent nephrotoxicity, as with radiolabeled somatostatin analogues.[45,46]

AUTHOR INFORMATION

Corresponding Author

*Anne Gruaz-Guyon, Inserm, U773, Faculté de Médecine Xavier Bichat, 16 rue Henri Huchard, BP 416, F-75018, France. E-mail: anne.gruaz-guyon@inserm.fr, Phone: (33) 1 57 27 75 55, Fax (33) 1 57 27 75 31.

Notes

[Δ]Faisal Alshoukr and Aurélie Prignon are to be considered as equal coauthors.

ACKNOWLEDGMENT

This work was supported by Inserm, by the Association pour la Recherche sur le Cancer (ARC), and by the Cancéropole Ile de France. We thank the Syrian government for awarding a research fellowship to F.A. We are grateful to Edouard Treca for IC_{50} determination of some peptides.

REFERENCES

(1) Myers, R. M., Shearman, J. W., Kitching, M. O., Ramos-Montoya, A., Neal, D. E., and Ley, S. V. (2009) Cancer, chemistry, and the cell: molecules that interact with the neurotensin receptors. *ACS Chem. Biol. 4*, 503–525.

(2) Vincent, J. P., Mazella, J., and Kitabgi, P. (1999) Neurotensin and neurotensin receptors. *Trends Pharmacol. Sci. 20*, 302–309.

(3) Evers, B. M. (2006) Neurotensin and growth of normal and neoplastic tissues. *Peptides 27*, 2424–2433.

(4) Thomas, R. P., Hellmich, M. R., Townsend, C. M., Jr., and Evers, B. M. (2003) Role of gastrointestinal hormones in the proliferation of normal and neoplastic tissues. *Endocr. Rev. 24*, 571–599.

(5) Ehlers, R. A., Kim, S., Zhang, Y., Ethridge, R. T., Murrilo, C., Hellmich, M. R., Evans, D. B., Townsend, C. M., Jr., and Mark Evers, B. (2000) Gut peptide receptor expression in human pancreatic cancers. *Ann. Surg. 231*, 838–848.

(6) Reubi, J. C., Waser, B., Friess, H., Buchler, M., and Laissue, J. (1998) Neurotensin receptors: a new marker for human ductal pancreatic adenocarcinoma. *Gut 42*, 546–550.

(7) Souaze, F., Dupouy, S., Viardot-Foucault, V., Bruyneel, E., Attoub, S., Gespach, C., Gompel, A., and Forgez, P. (2006) Expression of neurotensin and NT1 receptor in human breast cancer: a potential role in tumor progression. *Cancer Res. 66*, 6243–6249.

(8) Alifano, M., Souaze, F., Dupouy, S., Camilleri-Broet, S., Younes, M., Ahmed-Zaid, S. M., Takahashi, T., Cancellieri, A., Damiani, S., Boaron, M., Broet, P., Miller, L. D., Gespach, C., Regnard, J. F., and Forgez, P. (2010) Neurotensin receptor 1 determines the outcome of non-small cell lung cancer. *Clin. Cancer Res. 16*, 4401–4410.

(9) Alifano, M., Loi, M., Camilleri-Broet, S., Dupouy, S., Regnard, J. F., and Forgez, P. (2010) Neurotensin expression and outcome of malignant pleural mesothelioma. *Biochimie 92*, 164–170.

(10) Gui, X., Guzman, G., Dobner, P. R., and Kadkol, S. S. (2008) Increased neurotensin receptor-1 expression during progression of colonic adenocarcinoma. *Peptides 29*, 1609–1615.

(11) Shimizu, S., Tsukada, J., Sugimoto, T., Kikkawa, N., Sasaki, K., Chazono, H., Hanazawa, T., Okamoto, Y., and Seki, N. (2008) Identification of a novel therapeutic target for head and neck squamous cell carcinomas: a role for the neurotensin-neurotensin receptor 1 oncogenic signaling pathway. *Int. J. Cancer 123*, 1816–1823.

(12) Swift, S. L., Burns, J. E., and Maitland, N. J. (2010) Altered expression of neurotensin receptors is associated with the differentiation state of prostate cancer. *Cancer Res. 70*, 347–356.

(13) Reubi, J. C., Waser, B., Schaer, J. C., and Laissue, J. A. (1999) Neurotensin receptors in human neoplasms: high incidence in Ewing's sarcomas. *Int. J. Cancer 82*, 213–218.

(14) Dupouy, S., Viardot-Foucault, V., Alifano, M., Souaze, F., Plu-Bureau, G., Chaouat, M., Lavaur, A., Hugol, D., Gespach, C., Gompel, A., and Forgez, P. (2009) The neurotensin receptor-1 pathway contributes to human ductal breast cancer progression. *PLoS One 4*, e4223.

(15) Kwekkeboom, D. J., Kam, B. L., van Essen, M., Teunissen, J. J., van Eijck, C. H., Valkema, R., de Jong, M., de Herder, W. W., and Krenning, E. P. (2010) Somatostatin-receptor-based imaging and therapy of gastroenteropancreatic neuroendocrine tumors. *Endocr. Relat. Cancer 17*, R53–73.

(16) Krenning, E. P., Teunissen, J. J., Valkema, R., deHerder, W. W., deJong, M., and Kwekkeboom, D. J. (2005) Molecular radiotherapy with somatostatin analogs for (neuro-)endocrine tumors. *J. Endocrinol. Invest. 28*, 146–150.

(17) Granier, C., van Rietschoten, J., Kitabgi, P., Poustis, C., and Freychet, P. (1982) Synthesis and characterization of neurotensin analogues for structure/activity relationship studies. Acetyl-neurotensin-(8−13) is the shortest analogue with full binding and pharmacological activities. *Eur. J. Biochem. 124*, 117–124.

(18) Hillairet De Boisferon, M., Raguin, O., Thiercelin, C., Dussaillant, M., Rostene, W., Barbet, J., Pelegrin, A., and Gruaz-Guyon, A. (2002) Improved tumor selectivity of radiolabeled peptides by receptor and antigen dual targeting in the neurotensin receptor model. *Bioconjugate Chem. 13*, 654–662.

(19) Alshoukr, F., Rosant, C., Maes, V., Abdelhak, J., Raguin, O., Burg, S., Sarda, L., Barbet, J., Tourwe, D., Pelaprat, D., and Gruaz-Guyon, A. (2009) Novel neurotensin analogues for radioisotope targeting to neurotensin receptor-positive tumors. *Bioconjugate Chem. 20*, 1602–1610.

(20) Maecke, H. R., Hofmann, M., and Haberkorn, U. (2005) (68)Ga-labeled peptides in tumor imaging. *J. Nucl. Med. 46* (Suppl 1), 172S–178S.

(21) Wei, L., Zhang, X., Gallazzi, F., Miao, Y., Jin, X., Brechbiel, M. W., Xu, H., Clifford, T., Welch, M. J., Lewis, J. S., and Quinn, T. P. (2009) Melanoma imaging using (111)In-, (86)Y- and (68)Ga-labeled CHX-A″-Re(Arg11)CCMSH. *Nucl. Med. Biol. 36*, 345–354.

(22) Mansi, R., Wang, X., Forrer, F., Kneifel, S., Tamma, M. L., Waser, B., Cescato, R., Reubi, J. C., and Maecke, H. R. (2009) Evaluation of a 1,4,7,10-tetraazacyclododecane-1,4,7,10-tetraacetic acid-conjugated bombesin-based radioantagonist for the labeling with single-photon emission computed tomography, positron emission tomography, and therapeutic radionuclides. *Clin. Cancer Res. 15*, 5240–5249.

(23) Pagou, M., Zerizer, I., and Al-Nahhas, A. (2009) Can gallium-68 compounds partly replace (18)F-FDG in PET molecular imaging? *Hell. J. Nucl. Med. 12*, 102–105.

(24) Buchmann, I., Henze, M., Engelbrecht, S., Eisenhut, M., Runz, A., Schafer, M., Schilling, T., Haufe, S., Herrmann, T., and Haberkorn, U. (2007) Comparison of 68Ga-DOTATOC PET and 111In-DTPAOC (Octreoscan) SPECT in patients with neuroendocrine tumours. *Eur. J. Nucl. Med. Mol. Imaging 34*, 1617–1626.

(25) Hofmann, M., Maecke, H., Borner, R., Weckesser, E., Schoffski, P., Oei, L., Schumacher, J., Henze, M., Heppeler, A., Meyer, J., and Knapp, H. (2001) Biokinetics and imaging with the somatostatin receptor PET radioligand (68)Ga-DOTATOC: preliminary data. *Eur. J. Nucl. Med. 28*, 1751–1757.

(26) Gabriel, M., Decristoforo, C., Kendler, D., Dobrozemsky, G., Heute, D., Uprimny, C., Kovacs, P., Von Guggenberg, E., Bale, R., and Virgolini, I. J. (2007) 68Ga-DOTA-Tyr3-octreotide PET in neuroendocrine tumors: comparison with somatostatin receptor scintigraphy and CT. *J. Nucl. Med. 48*, 508–518.

(27) Kowalski, J., Henze, M., Schuhmacher, J., Macke, H. R., Hofmann, M., and Haberkorn, U. (2003) Evaluation of positron emission tomography imaging using [68Ga]-DOTA-D Phe(1)-Tyr(3)-Octreotide in comparison to [111In]-DTPAOC SPECT. First results in patients with neuroendocrine tumors. *Mol. Imaging Biol. 5*, 42–48.

(28) Liu, S. (2008) Bifunctional coupling agents for radiolabeling of biomolecules and target-specific delivery of metallic radionuclides. *Adv. Drug Delivery Rev. 60*, 1347–1370.

(29) Wang, D., Miller, S. C., Sima, M., Parker, D., Buswell, H., Goodrich, K. C., Kopeckova, P., and Kopecek, J. (2004) The arthrotropism of macromolecules in adjuvant-induced arthritis rat model: a preliminary study. *Pharm. Res. 21*, 1741–1749.

(30) Brans, L., Maes, V., Garcia-Garayoa, E., Schweinsberg, C., Daepp, S., Blauenstein, P., Schubiger, P. A., Schibli, R., and Tourwe, D. A. (2008) Glycation methods for bombesin analogs containing the (NalphaHis)Ac chelator for 99mTc(CO)3 radiolabeling. *Chem. Biol. Drug Des. 72*, 496–506.

(31) Raguin, O., Gruaz-Guyon, A., and Barbet, J. (2002) Equilibrium expert: an add-in to Microsoft Excel for multiple binding equilibrium simulations and parameter estimations. *Anal. Biochem. 310*, 1–14.

(32) Stefanovski, D., Moate, P. J., and Boston, R. C. (2003) WinSAAM: a windows-based compartmental modeling system. *Metabolism 52*, 1153–1166.

(33) Riches, A. C., Sharp, J. G., Thomas, D. B., and Smith, S. V. (1973) Blood volume determination in the mouse. *J. Physiol. 228*, 279–284.

(34) Sung, C., Youle, R. J., and Dedrick, R. L. (1990) Pharmacokinetic analysis of immunotoxin uptake in solid tumors: role of plasma kinetics, capillary permeability, and binding. *Cancer Res. 50*, 7382–7392.

(35) Covell, D. G., Barbet, J., Holton, O. D., Black, C. D., Parker, R. J., and Weinstein, J. N. (1986) Pharmacokinetics of monoclonal immunoglobulin G1, F(ab′)2, and Fab′ in mice. *Cancer Res. 46*, 3969–3978.

(36) Akizawa, H., Arano, Y., Mifune, M., Iwado, A., Saito, Y., Mukai, T., Uehara, T., Ono, M., Fujioka, Y., Ogawa, K., Kiso, Y., and Saji, H. (2001) Effect of molecular charges on renal uptake of 111In-DTPA-conjugated peptides. *Nucl. Med. Biol. 28*, 761–768.

(37) Froidevaux, S., Calame-Christe, M., Tanner, H., and Eberle, A. N. (2005) Melanoma targeting with DOTA-alpha-melanocyte-stimulating hormone analogs: structural parameters affecting tumor uptake and kidney uptake. *J. Nucl. Med. 46*, 887–895.

(38) Barroso, S., Richard, F., Nicolas-Etheve, D., Reversat, J. L., Bernassau, J. M., Kitabgi, P., and Labbe-Jullie, C. (2000) Identification of

residues involved in neurotensin binding and modeling of the agonist binding site in neurotensin receptor 1. *J. Biol. Chem. 275*, 328–336.

(39) Garcia-Garayoa, E., Blauenstein, P., Blanc, A., Maes, V., Tourwe, D., and Schubiger, P. A. (2009) A stable neurotensin-based radiopharmaceutical for targeted imaging and therapy of neurotensin receptor-positive tumours. *Eur. J. Nucl. Med. Mol. Imaging 36*, 37–47.

(40) Maes, V., Garcia-Garayoa, E., Blauenstein, P., and Tourwe, D. (2006) Novel 99mTc-labeled neurotensin analogues with optimized biodistribution properties. *J. Med. Chem. 49*, 1833–1836.

(41) Achilefu, S., Srinivasan, A., Schmidt, M. A., Jimenez, H. N., Bugaj, J. E., and Erion, J. L. (2003) Novel bioactive and stable neurotensin peptide analogues capable of delivering radiopharmaceuticals and molecular beacons to tumors. *J. Med. Chem. 46*, 3403–3411.

(42) de Visser, M., Janssen, P. J., Srinivasan, A., Reubi, J. C., Waser, B., Erion, J. L., Schmidt, M. A., Krenning, E. P., and de Jong, M. (2003) Stabilised 111In-labelled DTPA- and DOTA-conjugated neurotensin analogues for imaging and therapy of exocrine pancreatic cancer. *Eur. J. Nucl. Med. Mol. Imaging 30*, 1134–1139.

(43) Froidevaux, S., Eberle, A. N., Christe, M., Sumanovski, L., Heppeler, A., Schmitt, J. S., Eisenwiener, K., Beglinger, C., and Macke, H. R. (2002) Neuroendocrine tumor targeting: study of novel gallium-labeled somatostatin radiopeptides in a rat pancreatic tumor model. *Int. J. Cancer 98*, 930–937.

(44) Koumarianou, E., Mikolajczak, R., Pawlak, D., Zikos, X., Bouziotis, P., Garnuszek, P., Karczmarczyk, U., Maurin, M., and Archimandritis, S. C. (2009) Comparative study on DOTA-derivatized bombesin analog labeled with 90Y and 177Lu: in vitro and in vivo evaluation. *Nucl. Med. Biol. 36*, 591–603.

(45) de Jong, M., Rolleman, E. J., Bernard, B. F., Visser, T. J., Bakker, W. H., Breeman, W. A., and Krenning, E. P. (1996) Inhibition of renal uptake of indium-111-DTPA-octreotide in vivo. *J. Nucl. Med. 37*, 1388–1392.

(46) Vegt, E., van Eerd, J. E., Eek, A., Oyen, W. J., Wetzels, J. F., de Jong, M., Russel, F. G., Masereeuw, R., Gotthardt, M., and Boerman, O. C. (2008) Reducing renal uptake of radiolabeled peptides using albumin fragments. *J. Nucl. Med. 49*, 1506–1511.